Supplemental Material

Section 1: The Cartesian multipolar decomposition

The current density $\vec{J}$ can be obtained from the formula $\vec{J}=-i\omega\varepsilon_0(n^2-1)\vec{E}$, all multipole moments can be defined as [R1] [R2]:

$$\vec{P}=\frac{1}{i\omega}\int\vec{J}d^3r, \tag{S1}$$

$$\vec{M}=\frac{1}{2c}\int(\vec{r}\times\vec{J})d^3r, \tag{S2}$$

$$\vec{T}=\frac{1}{10c}\int[(\vec{r}\cdot\vec{J})\vec{r}-2r^2\vec{J}]d^3r, \tag{S3}$$

$$Q^{(e)}_{\alpha\beta}=\frac{1}{2i\omega}\int[r_\alpha J_\beta+r_\beta J_\alpha-\frac{2}{3}(\vec{r}\cdot\vec{J})\delta_{\alpha,\beta}]d^3r, \tag{S4}$$

$$Q^{(m)}_{\alpha\beta}=\frac{1}{3c}\int[[\vec{r}\times\vec{J}]_\alpha r_\beta+[\vec{r}\times\vec{J}]_\beta r_\alpha]d^3r, \tag{S5}$$

Where $\vec{r}$ is the displacement vector from the origin to the specific point (x, y, z), c and ω are the speed and angular frequency of light, respectively, and α, $\beta=x, y, z$. The $\vec{P}$, $\vec{Q}^{(e)}$, $\vec{M}$, $\vec{Q}^{(m)}$, $\vec{T}$ are the electric dipole (ED) moment, electric quadrupole (EQ) moment, magnetic dipole (MD) moment, magnetic quadrupole (MQ) moment and toroidal dipole (TD) moment, respectively. The distributed powers of these multipole moments are calculated as follow:

$$I_p=\frac{2\omega^4}{3c^3}|\vec{P}|^2, \tag{S6}$$

$$I_{Q^{(e)}}=\frac{\omega^6}{5c^5}\sum|\vec{Q}^{(e)}_{\alpha\beta}|^2, \tag{S7}$$

$$I_M=\frac{2\omega^4}{3c^3}|\vec{M}|^2, \tag{S8}$$

$$I_{Q^{(m)}}=\frac{\omega^6}{40c^5}\sum|\vec{Q}^{(m)}_{\alpha\beta}|^2, \tag{S9}$$

$$I_T=\frac{2\omega^6}{3c^5}|\vec{T}|^2. \tag{S10}$$

Section 2: Comparison of Si-Graphene composite metasurface's transmission curves at different Fermi levels

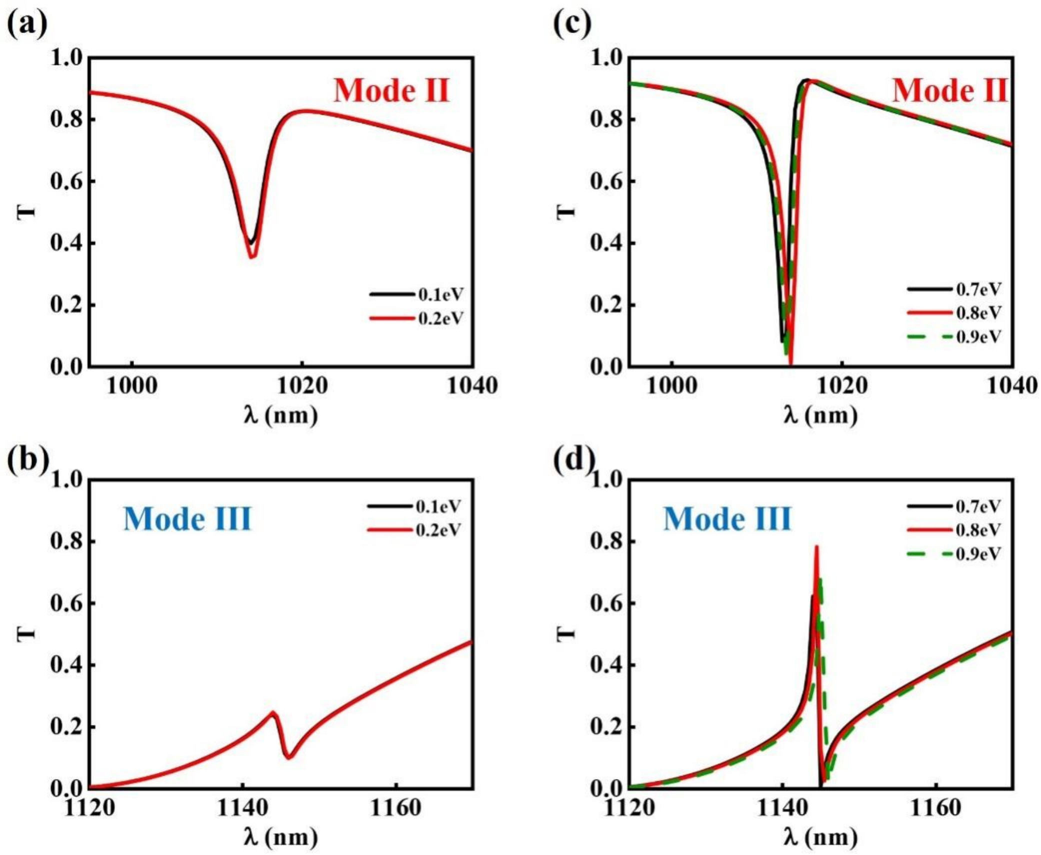

Fig. S1. Comparison of transmission curves at E_F = 0.1 and 0.2 eV in (a) Mode II, (c) Mode III. Comparison of transmission curves at E_F = 0.7, 0.8 and 0.9 eV in (b) Mode II, (d) Mode III.

Section 3: The simulated and the theory transmission curves of Si-Graphene composite metasurface at E_F = 0.1 and 0.8 eV

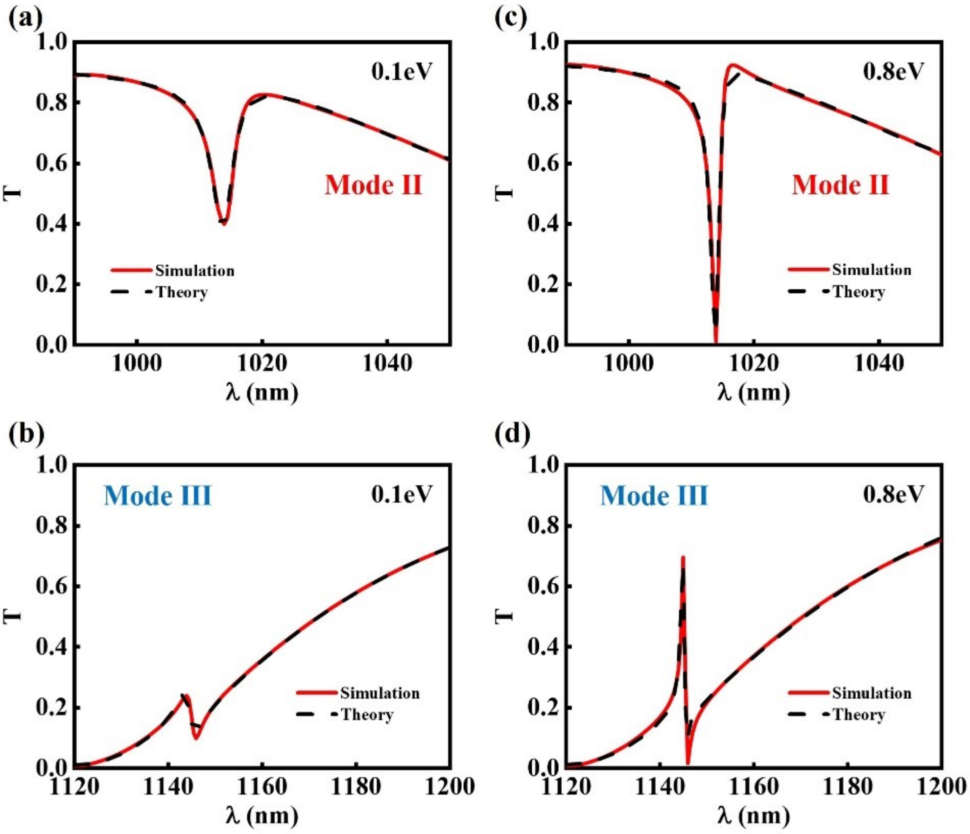

Fig. S2. Simulated (solid red line) and theory (black dotted line) transmission curves of the Si-Graphene composite metasurface at E_F = 0.1 eV in (a) Mode II, (b) Mode III. Simulated (solid red line) and theory (black dotted line) transmission curves of the Si-Graphene composite metasurface at E_F = 0.8 eV in (c) Mode II, (d) Mode III.

Section 4: The multipolar decomposition of Si-Graphene composite metasurface

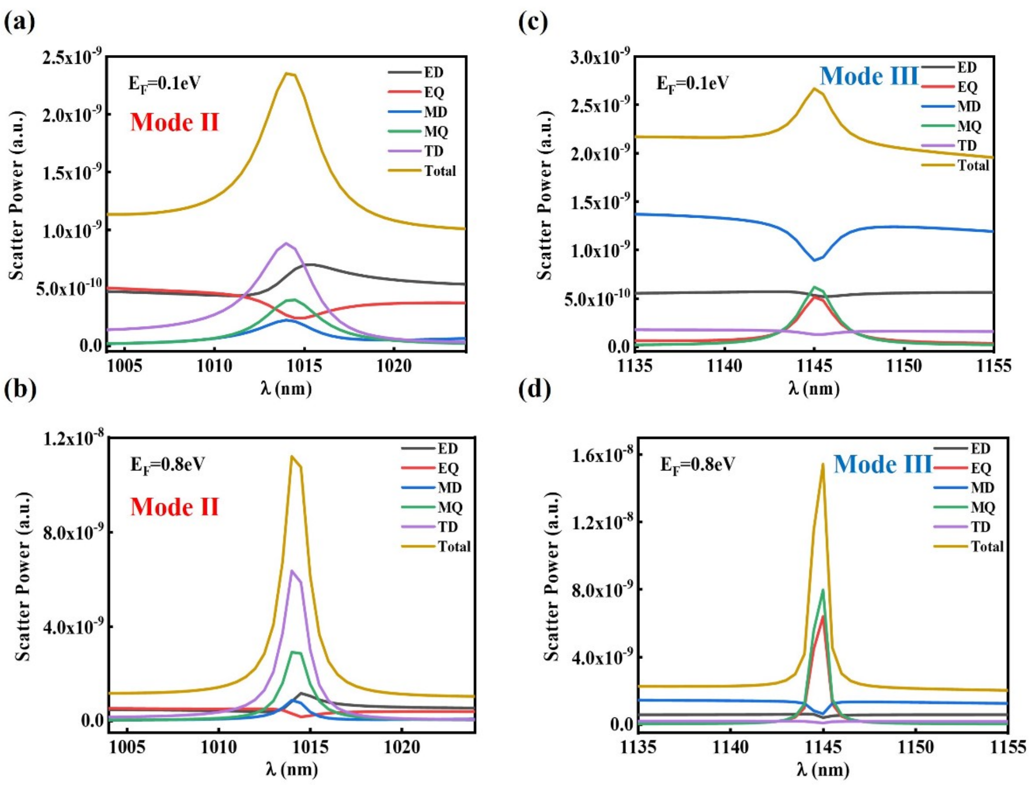

Fig. S3. Multipolar decomposition for the scattering power of the Si-graphene composite metasurface at E_F =0.1eV in (a) Mode II, (c) Mode III. Multipolar decomposition for the scattering power of the Si-graphene composite metasurface at E_F =0.8eV in (a) Mode II, (c) Mode III.

Section 5: The optical material losses of Si-Graphene composite metasurface

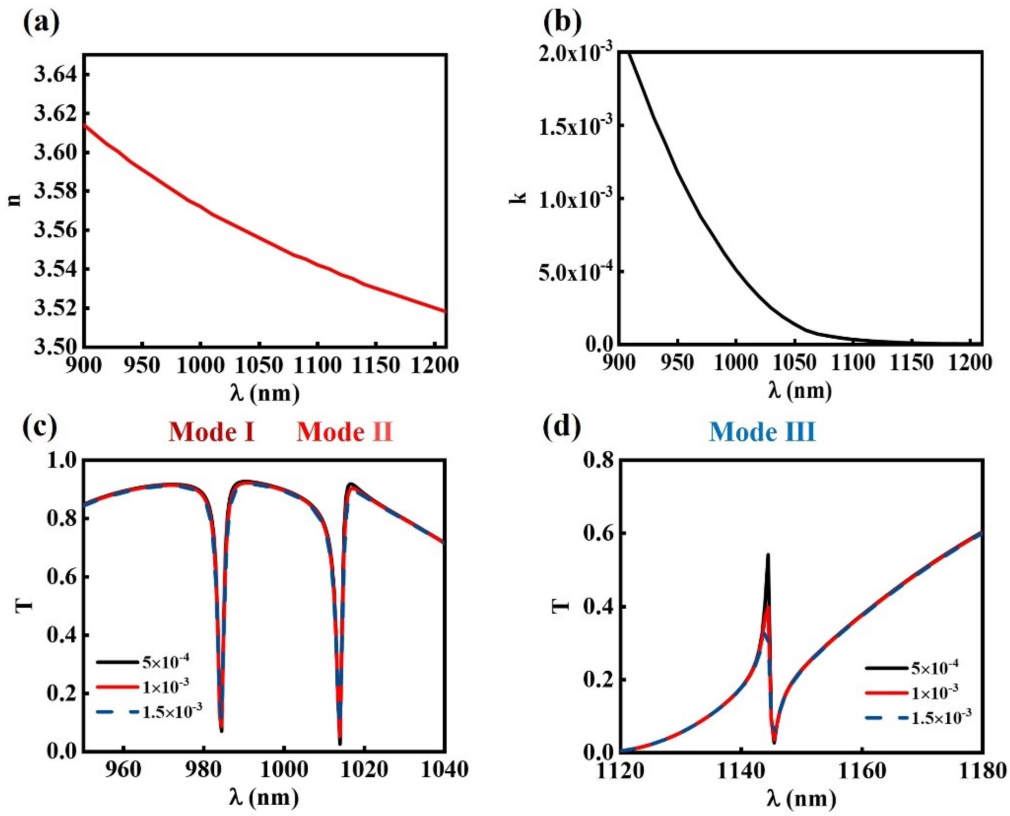

Fig. S4. (a) The real part of the refractive index *n* and (b) the imaginary part of the refractive index *k* of Si under the wavelength of 900nm–1210nm. Transmission spectrum at different loss levels (*k*) of the Si-graphene composite metasurface at E_F =0.8eV in (c) Mode I, Mode II, (d) Mode III.

As for the proposed composite metasurface, the material losses of silicon will introduce the absorption and scattering losses, which will affect the optical characteristics of Si-graphene composite metasurface. Here, the extinction coefficient k, the imaginary part of the silicon refractive index, is employed to quantify the material losses, so we have calculated the transmission spectra of Si-Graphene composite metasurface at different loss levels (k). Figs. S4. (a) and (b) are the real part and the imaginary part of the refractive index k of silicon under the studied wavelength. Figs. S4. (c) and (d) are the transmission spectrums at different loss levels (k) of the Si-graphene composite metasurface at E_F =0.8eV in Mode I, Mode II and Mode III. When the k increases, the transmission waveform deteriorates gradually. The transmission in Mode III is the most sensitive to the material losses, and its extremum value and Q-factor decrease obviously when k >10^{-3}. However, the transmission in Mode I and Mode II are affected slightly.

[R1] C. Zhou, S. Li, Y. Wang, M. Zhan, Multiple toroidal dipole Fano resonances of asymmetric dielectric nanohole arrays, Physical Review B. 100 (19) (2019) 195306. https://doi.org/10.1103/PhysRevB.100.195306.

[R2] V. Savinov, V.A. Fedotov, N.I. Zheludev, Toroidal dipolar excitation and macroscopic electromagnetic properties of metamaterials, Physical Review B. (20) (2014) 205112, http://dx.doi.org/10.1103/PhysRevB.89.205112.